Molecular Therapy
Methods & Clinical Development
Original Article

Adeno-Associated Viral Vector 2 and 9 Transduction Is Enhanced in Streptozotocin-Induced Diabetic Mouse Retina

Si Hyung Lee,[1,2,5] Jin Young Yang,[2,3,5] Sanjar Madrakhimov,[2,3] Ha Yan Park,[2] Keerang Park,[4] and Tae Kwann Park[1,2]

[1]Department of Ophthalmology, College of Medicine, Soonchunhyang University, Cheonan 31151, Republic of Korea; [2]Department of Ophthalmology, Soonchunhyang University Hospital Bucheon, Bucheon 14584, Republic of Korea; [3]Department of Biomedical Science, Graduate School, Soonchunhyang University, Asan 31538, Republic of Korea; [4]Department of Biopharmacy, Chungbuk Health & Science University, Cheongju, Chungbuk 28150, Republic of Korea

Adeno-associated viruses (AAVs) are currently the most popular vector platform technology for ocular gene therapy. While transduction efficiency and tropism of intravitreally administered AAV has been fairly well established in various retinal conditions, its transduction pattern in diabetic retinas has not previously been characterized. Here, we describe the transduction efficiencies of four different AAV serotypes, AAV2, 5, 8, and 9, in streptozotocin (STZ)-induced diabetic mouse retinas after intravitreal injections, which differed according to the duration of diabetic induction. STZ was intraperitoneally injected into C57/B6 diabetic mice subjected to unilateral intravitreal injection of AAV2, AAV5, AAV8, and AAV9 packaged with EGFP. Significantly enhanced AAV2 and AAV9 transduction was observed in 2-month-old diabetic mouse retinas compared to the 2-week-old diabetic mouse retinas and nondiabetic, vector uninjected or injected retinas. Intravitreal injection of AAV5 or AAV8 serotype in 2-month- and 2-week-old diabetic mouse retinas did not show any significant vector transduction enhancement compared to the nondiabetic control retinas. The tropism of AAV2 and AAV9 in diabetic mouse retinas differed. AAV2 was transduced into various retinal cells, including Müller cells, microglia, retinal ganglion cells (RGCs), bipolar cells, horizontal cells, and amacrine cells, whereas AAV9 was effectively transduced only into RGC and horizontal cells. The expression levels of receptors and co-receptors for AAV2 and AAV9 were significantly increased in 2-month-old diabetic mouse retinas. The results of our study demonstrated that AAV2 and AAV9 may be the vector of choice in treating diabetic retinopathy (DR) with gene therapy, and DR-related retinal changes may improve AAV vector transduction efficiency.

INTRODUCTION

Diabetic retinopathy (DR) is a chronic progressive disease of the retinal microvasculature associated with prolonged hyperglycemia. Uncontrolled hyperglycemia may lead to proliferative DR (PDR) and diabetic macular edema (DME), which are sight-threatening complications of DR. Pan-retinal photocoagulation has been the standard treatment for PDR since a report from the Diabetic Retinopathy Study,[1] but side effects of laser treatment, such as a decreased peripheral visual field and night vision, are still a concern.[2,3] After the introduction of anti-vascular endothelial growth factor (VEGF) therapy, intravitreal injection of anti-VEGF agents has been the main treatment for DME.[4] However, monthly treatments and the risk of ocular infection or other complications are burdensome to patients. Therefore, there is a need to develop new therapeutic modalities to overcome such limitations. One possible candidate that could replace current therapies for DR is ocular gene therapy, which could deliver more sustained and long-lasting therapeutic effects.

Adeno-associated virus (AAV) is one of the most widely used and promising delivery methods for ocular gene therapy. AAV-based ocular gene therapy has proven effective for the treatment of blinding retinal diseases, such as Leber congenital amaurosis (LCA),[5–7] and numerous clinical studies are in progress to determine its potential therapeutic effects in other retinal diseases.[8–12] It was previously reported that intravitreal or subretinal administration of different serotypes of AAV may transduce genes into specific cell types of the neural retina, from retinal ganglion cells (RGCs) to deep-lying photoreceptor cells.[13–15] Although the tropisms of AAV serotypes for retinal cells are fairly well established, the tropism may change according to the pathological state of the retina;[14,16,17] thus, identifying the most appropriate serotype for each retinal disease is the next important step before beginning to evaluate the therapeutic effects of this novel therapy.

Several previous studies have shown the feasibility of using ocular genes for the treatment of DR, demonstrating specific therapeutic effects using the AAV2 vector encoding inhibitors of vasopermeability, such as the soluble VEGF receptor 1 (*sFlt-1*),[18] vasoinhibin,[19]

Received 12 October 2018; accepted 25 November 2018;
https://doi.org/10.1016/j.omtm.2018.11.008.

[5]These authors contributed equally to this work.

Correspondence: Tae Kwann Park, MD, PhD, Department of Ophthalmology, Soonchunhyang University Hospital Bucheon, 170 Jomaru-ro, Wonmi-gu, Bucheon 14584, Republic of Korea.
E-mail: tkpark@schmc.ac.kr

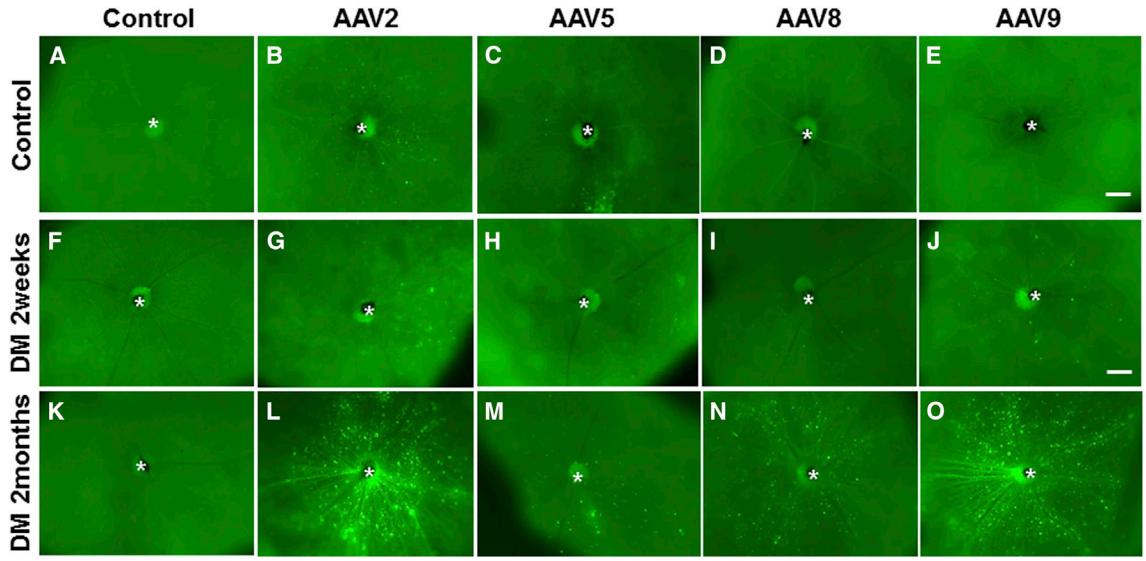

Figure 1. Fundus Fluorescent Images of Control Mice and 2-Week- and 2-Month-Old Diabetic Mice

The fundi of the nondiabetic control (A) and diabetic mice without vector administration at 2 weeks (F) and 2 months (K) showed scant background autofluorescence. Occasional scattered EGFP expression was observed in adeno-associated virus (AAV) 2 (B), 5 (C), 8 (D), and 9 (E)-injected-nondiabetic retinas and AAV2-injected eyes showing the highest fluorescence. In the fundi of 2-week-old diabetic mice, similar EGFP expression to that of nondiabetic mice fundi was observed in AAV 2 (G), 5 (H), 8 (I), and 9 (J) serotypes. Two months of STZ injection induced markedly increased transduction throughout the fundi in AAV2- (L) and AAV9 (O)-administered eyes, while modest EGFP expression was detected in AAV5- (M) and AAV8- (N) injected eyes.

angiostatin,[20] and angiotensins.[21] Also, a recent study reported enhanced AAV2 transduction in diabetic rat retinas, due to enhanced cell entrance upon diabetic retinal changes.[16] However, other AAV serotypes, such as AAV5, AAV8, and AAV9, have not previously been evaluated. While targeted ocular gene therapy may be possible for all types of retinal cell, it is important to evaluate viral tropism of different AAV serotypes in retinas with DR. Moreover, differences in retinal vascular and structural changes according to DR stage may also contribute to alterations to viral vector tropism, which have never previously been investigated. Investigating the retinal transduction of AAV in eyes with DR at different times after hyperglycemia induction is therefore necessary to evaluate its therapeutic utility in the treatment of DR.

Based on these considerations, we investigated different transduction patterns of four AAV serotypes, AAV2, AAV5, AAV8, and AAV9, in the retinas of 2-week- or 2-month-old streptozotocin (STZ)-induced diabetic mice. We determined the specific tropisms of the four AAV serotypes in different retinal layers and cells, as well as the expression levels of the relevant receptors for AAVs.

RESULTS

Different Transduction Efficacies of AAV Serotypes in Diabetic Mouse Fundi

Only weak background autofluorescence was observed in nondiabetic and diabetic fundi without AAV administration (Figures 1A, 1F, and 1K), while a few scattered regions of EGFP expression were observed in AAV-injected nondiabetic eyes, indicating that the AAV2 vector was the most efficiently transduced, as reported previously (Figures 1B–1E).[14] In diabetic mice fundi after 2 weeks of STZ injection, similar EGFP expression patterns to those of nondiabetic eyes were detected for all four AAV serotypes (Figures 1F–1J). Among eyes from mice after 2 months of STZ injection, markedly increased EGFP expression throughout the fundi was noted in AAV2- and AAV9-injected eyes (Figures 1L and 1O), while AAV5- and AAV8-injected eyes showed modest EGFP expression levels (Figures 1M and 1N). The quantitatively measured fluorescence intensity was significantly stronger in all four of the AAV serotypes that were injected into control eyes when compared to uninjected control eyes (AAV2, $p = 0.015$; AAV5, $p = 0.043$; AAV8, $p = 0.037$; and AAV9, $p = 0.023$). Two-week-old diabetic mice fundi after AAV administration also showed significantly increased fluorescence intensity compared to control eyes without vector administration, irrespective of the AAV serotype (AAV2, $p = 0.005$; AAV5, $p = 0.045$; AAV8, $p = 0.042$; and AAV9, $p = 0.021$) but did not show significantly different fluorescence intensities compared to AAV-injected nondiabetic eyes (AAV2, $p = 0.085$; AAV5, $p = 0.153$; AAV8, $p = 0.242$; and AAV9, $p = 0.121$). Among diabetic mice after 2 months of STZ treatment, all eyes injected with each of the four serotypes showed significantly increased fluorescence intensity compared to that of the uninjected eyes in nondiabetic mouse retinas (AAV2, $p < 0.001$; AAV5, $p = 0.012$; AAV8, $p = 0.003$; and AAV9, $p < 0.001$). However, when compared to vector-injected, nondiabetic eyes, only AAV2- and AAV9-administered eyes showed significantly increased fluorescence intensity (AAV2, $p = 0.028$; and AAV9, $p = 0.032$), while AAV5- and AAV8-injected eyes demonstrated

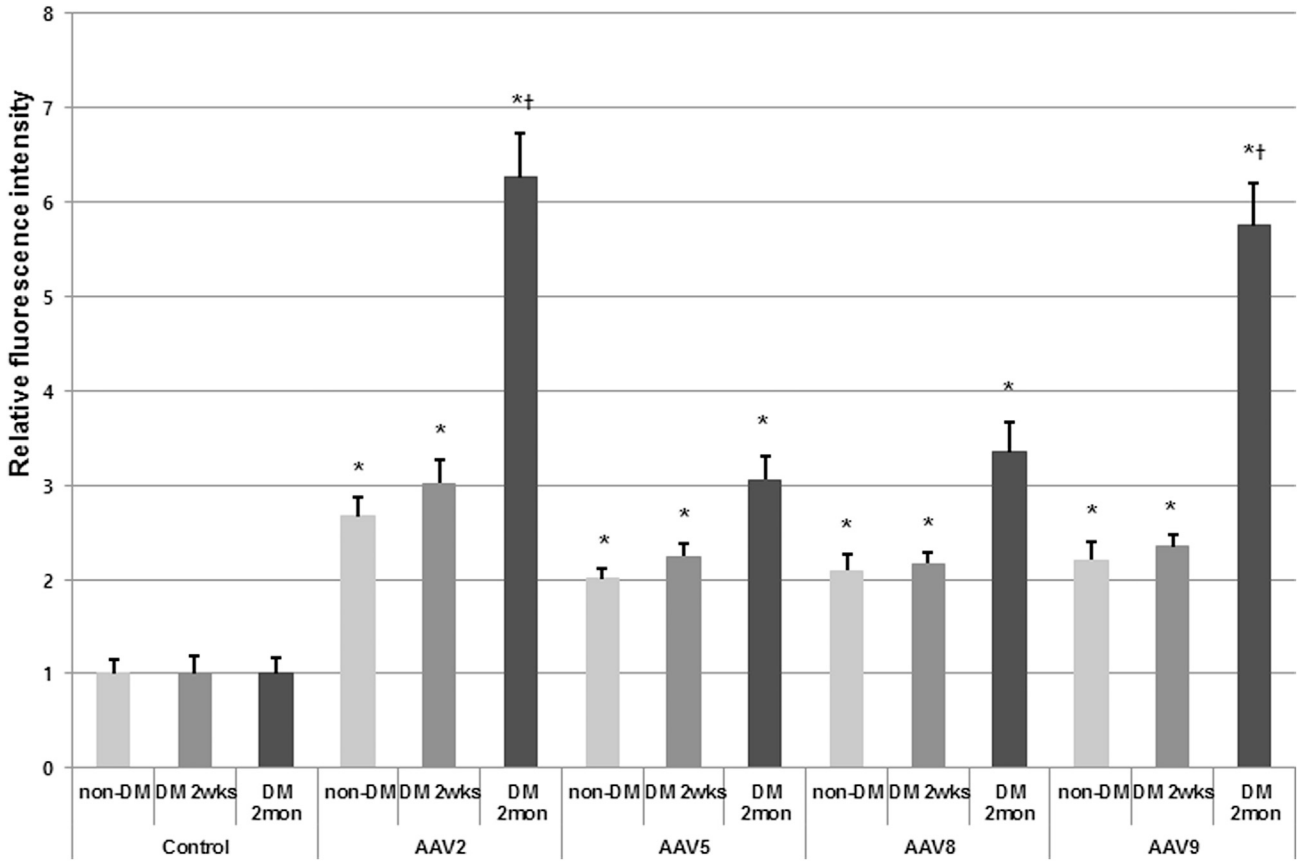

Figure 2. Quantitative Analyses of Relative Fluorescence Intensity: Comparison between the Control and 2-Week- and 2-Month-Old Diabetic Mice with Different Serotypes

The measured relative fluorescence intensity was significantly stronger in all four AAV-serotype-injected nondiabetic control eyes compared to uninjected, nondiabetic eyes (AAV2, $p = 0.015$; AAV5, $p = 0.043$; AAV8, $p = 0.037$; and AAV9, $p = 0.023$), and the fluorescence intensity in 2-week-old diabetic mouse fundi with AAV administration was also similar to AAV-injected, nondiabetic eyes (AAV2, $p = 0.085$; AAV5, $p = 0.153$; AAV8, $p = 0.242$; and AAV9, $p = 0.121$ compared to AAV2-, AAV5-, AAV8-, and AAV9-injected nondiabetic eyes, respectively). Significantly increased intensity was observed in AAV-injected, 2-month-old diabetic mouse retinas compared to that of AAV-uninjected, nondiabetic mouse retinas (AAV2, $p < 0.001$; AAV5, $p = 0.012$; AAV8, $p = 0.003$; and AAV9, $p < 0.001$), and diabetic mouse eyes with AAV2 and AAV9 administration showed significantly increased fluorescence intensity compared to AAV-injected, nondiabetic mouse eyes (AAV2, $p = 0.028$; AAV9, $p = 0.032$). Data are expressed as the mean ± SEM. *$p < 0.05$ compared to the uninjected, nondiabetic group, tested by the Mann-Whitney U test. †$p < 0.05$, compared to 2-week-old diabetic mice, tested by the Mann-Whitney U test.

nonsignificant, but mild increase in fluorescence intensity (AAV, $p = 0.075$ and AAV8, $p = 0.068$) (Figure 2).

AAV Transduction in Various Retinal Layers in Diabetic Mice

Because AAV2 and AAV9 serotypes showed significantly enhanced transduction capacities in whole-mount examinations, the two AAV serotype-injected eyes were further evaluated using transverse retinal sections. In the AAV2-injected eyes, nondiabetic mouse eyes demonstrated clear EGFP expression, mainly in the superficial layers of the retina, the retinal nerve fiber layer (RNFL), the RGCs, and, sporadically, in the inner nuclear layer (INL) (Figure 3A). After 2 months of STZ injection, diffuse vector transduction was seen in the RNFL and RGCs, as well as in the inner plexiform layer (IPL), and the INL was markedly enhanced compared to the control AAV2-injected eyes (Figure 3C). In AAV9-injected, nondiabetic eyes, EGFP expression was almost negligible in all retinal layers (Figure 3B). In 2-month-old diabetic mouse retinas, similar transduction patterns were observed to those seen in AAV2-injected diabetic eyes, involving transduced cells in the RNFL and RGC layer, together with cells in the INL and axons in the IPL (Figure 3D).

Effective AAV Transduction into Different Retinal Cells in Diabetic Retinas

In AAV2-injected eyes, many EGFP-positive cells co-localized with various cell markers. Co-localization of EGFP and glutamine synthetase (GS) expression showed effective vector transduction in Müller cells in AAV2-injected diabetic mouse retinas (Figures 4A–4B), whereas the expression of CD31, a marker for endothelial cells, was detected mainly in the inner retinal layers, which did not co-localize with any EGFP-positive cells (Figures 4C–4D). A few cells positive for

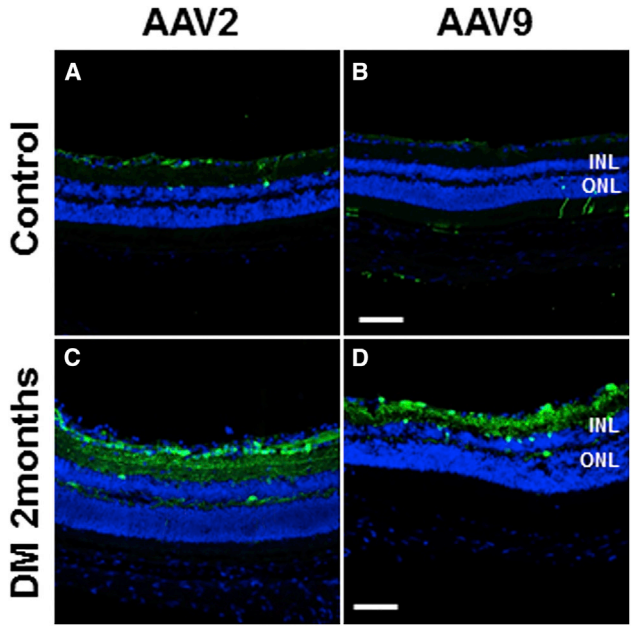

Figure 3. Transverse Retinal Sections Showing EGFP Expression Patterns in Nondiabetic Controls and 2-Month-Old Diabetic Mice after Intravitreal Injection of AAV2 or AAV9

Upon intravitreal AAV2 administration, nondiabetic mouse eyes demonstrated sporadic EGFP expression mainly in the retinal nerve fiber layer (RNFL), retinal ganglion cell (RGC) layer, and inner nuclear layer (INL) (A). A transverse section of 2-month-old diabetic mouse retinas revealed markedly enhanced vector transduction in the RNFL and RGC, as well as in the INL (C). In AAV9-injected eyes, nondiabetic mouse retinas showed limited transduction (B), while 2-month-old diabetic mouse retinas showed enhanced transduction in the RNFL, RGC layer, and INL, similar to the pattern seen in AAV2-injected diabetic mouse eyes (D). ONL, outer nuclear layer. Scale bar, 100 μm.

iba-1, a microglia marker, were observed in the inner retinal layer, and some of them co-localized with EGFP (Figures 4E–4F). As seen in Figure 3, EGFP expression was most abundant in the RGC layers in 2-month-old diabetic mouse retinas, and many EGFP-positive cells co-localized with NeuN expression in both AAV2-injected diabetic mouse retinas (Figures 4G–4H). Protein kinase-C α (PKCα) (Figures 4I–4J), calbindin (Figures 4K–4L), and calretinin (Figures 4M–4N) also co-localized with EGFP, suggesting that AAV2 was effectively transduced into various structural cells, including RGCs, bipolar cells, amacrine cells, and horizontal cells, which constituted the inner retinal layers in diabetic mouse retinas.

AAV9-injected diabetic mouse retinas showed rather limited transduction compared to those injected with AAV2 in transverse retinal sections. Müller cell transduction was observed in glutamine synthetase (GS)-co-stained sections (Figures 5A–5B), while CD31 (Figures 5C–5D) and iba-1 staining (Figures 5E–5F) did not reveal any co-localization with EGFP expression. EGFP-positive cells also co-localized with NeuN (Figures 5G–5H) and calbindin (Figures 5K–5L), indicating effective transduction in RGCs and horizontal cells. However, PKCα and calretinin staining did not reveal any co-localization with EGFP (Figures 5I–5J and 5M–5N).

Increased Expression of Primary and Co-receptors Related to AAV2 and AAV9 in Diabetic Retinas

The expression levels of syndecan-4, glypican-1, and all three co-receptors for AAV2 were significantly increased in diabetic mouse retinas compared to normal controls, whereas the perlecan-1 levels were significantly decreased in diabetic mouse retinas (Figures 6A and 6B). Consistent with the results of qRT-PCR, immunostaining of perlecan-1 revealed localized immunoreactivity only in superficial retinal layers, which was the same as that in nondiabetic mouse retinas (Figure 6C and 6D); the expression of syndecan-4 was significantly upregulated in diabetic mouse retinas, especially in the INL (Figures 6E and 6F). Regarding the AAV9 receptors, the mRNA levels of the 37- and 67-kDa laminin receptors were also significantly enhanced in diabetic mouse retinas compared to the controls (Figure 7A). Similarly, immunoreactivity of the 37- and 67-kDa laminin receptors in diabetic mouse retinas were markedly enhanced compared to nondiabetic mouse retinas, both in the RNFL and RGC layers and in the INL (Figures 7B and 7C). The expression of Ricinus Communis Agglutinin I (RCA I) was also increased, mostly in the superficial retinal layers, of diabetic mouse retinas (Figures 7D and 7E).

Vascular Changes and Glial Activation in Diabetic Retinas

When vascular density was analyzed using retinal whole mounts with CD31 staining, the avascular area was markedly increased in diabetic mouse retinas after 2 months of STZ treatment compared to those observed in the normal control and mouse retinas of 2 weeks of diabetes (Figure 8A–8C). Moreover, increased GFAP (Figure 8D–8F) and iba-1 (Figure 8G–8I) expressions were detected in mouse retinas of 2 months' duration of diabetes compared to the normal and 2-week-old diabetic mouse retina, indicating increased glial responses.

DISCUSSION

Following the first successful clinical trial with AAV in LCA patients,[5] various retinal pathological conditions have been considered as possible candidates for ocular gene therapy, including DR. A previous study evaluated AAV transduction efficiencies in diabetic retinas, but using only AAV2 serotypes.[16] In this study, using four different serotypes, AAV2, AAV5, AAV8, and AAV9, we demonstrated that transduction enhancement was achieved in the mouse retinas of 2 months' duration of diabetes with the AAV2 and AAV9 serotypes. Vector transduction was mostly observed in retinal cells located in the inner retina, as shown by immunohistochemical analyses using various antibodies, and receptors related to AAV2 and AAV9 were also significantly increased in diabetic mouse retinas.

Enhanced vector transduction was observed mainly in the inner retinal layer, both in AAV2- and AAV9-injected diabetic mouse retinas. Transverse retinal sections further revealed more diverse transduction patterns in AAV2-injected diabetic mouse retinas when compared to retinas injected with AAV9. Immunostaining

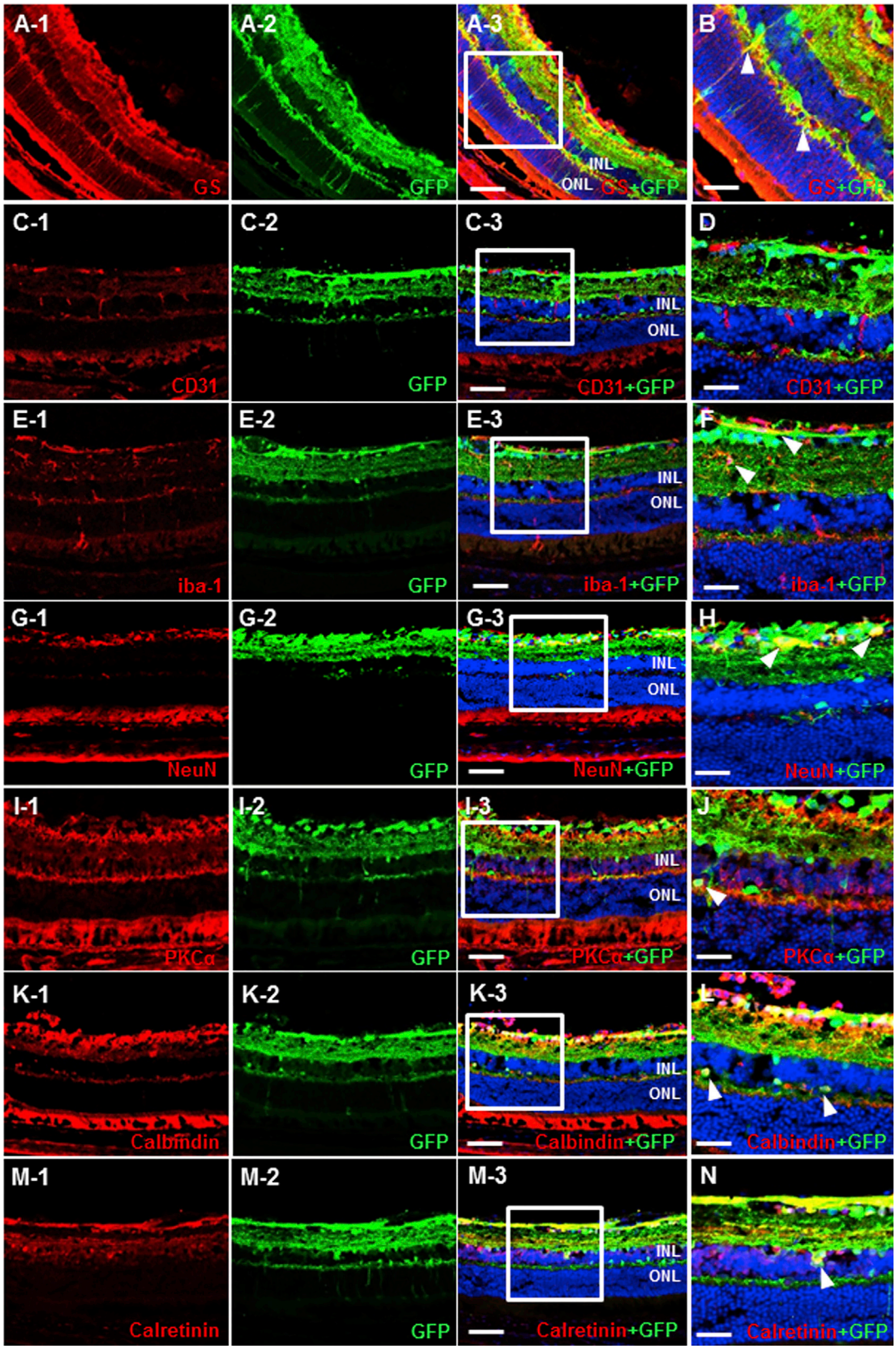

(legend on next page)

for various retinal cell markers showed that the targeted retinal cells differed between AAV2- and AAV9-injected diabetic eyes; AAV2 was effectively transduced into RGCs, amacrine cells, bipolar cells, horizontal cells, Müller cells, and microglia, while AAV9 was only transduced into some of the RGCs, Müller cells, and a few horizontal cells. While the different tropisms of AAV serotypes between normal and other pathological retinas were fairly well established in previous studies,[14,22–27] there has been no report regarding the AAV serotype tropisms in eyes with DR. The results from our study provide further guidance for selecting the most-appropriate AAV serotype when considering targeted ocular gene therapy to treat DR and its related complications.

One of the interesting findings of this study was that transduction of AAV2 and AAV9 were significantly enhanced in 2-month-old diabetic mice, but not in 2-week-old diabetic mice. This result suggests that immediate hyperglycemia or the chemical effect of STZ itself may not be responsible for the AAV transduction enhancement in the mouse retina. Also, although statistically not significant, AAV5- and AAV8-injected 2-month-old diabetic mice showed mildly increased vector transduction compared to the nondiabetic control and 2-week-old diabetic mice. While it takes time for the DR-related retinal structural and/or vascular pathological changes to occur, it can be assumed that actual retinal structural changes may be closely related with such enhanced vector transduction. To confirm this hypothesis, we investigated whether there are vascular and glial changes at 2-weeks' and 2-months' duration of diabetes using retinal whole mounts and transverse sections and demonstrated that avascular retinal areas and glial activity were markedly increased at 2 months of diabetes compared to the control and 2 weeks of diabetes. Previous studies have reported that subclinical microangiopathy, such as decreased retinal blood flow and blood-retinal barrier breakdown, may occur after 1–2 weeks in STZ-induced diabetic animals.[28–31] While our results did not show significant changes in AAV2 or AAV9 transduction in diabetic mouse retinas at 2 weeks' duration of diabetes, it is probable that simple hyperglycemic and subclinical vascular changes may not have any effect on the enhancement of vector transduction in the diabetic retinas. Increased glial cell responses prominent in 8- to 10-week-old STZ-induced diabetic animals, as shown in our study, may have played a significant role in the AAV transduction efficiency of diabetic retinas.[32,33] Moreover, our results demonstrated that enhanced AAV transduction was mostly localized in the INL, consistent with previous studies reporting that structural changes related to early DR occur predominantly in the inner retina. Retinal neuroglial abnormalities have been observed in the inner retina during early phases of DR,[34–36] and inner retinal abnormalities have been observed in STZ-induced diabetic rats as early as 4–8 weeks.[37] Along with these previous reports, retinal vascular and neuroglial changes shown in our study further support the increased vector transduction observed in mouse retinas at 2 months of diabetes.

Several receptors have previously been identified as being directly or indirectly related to the AAV2 transduction mechanism. Heparan sulfate proteoglycans (HSPGs) are glycoproteins found on cell membranes and the extracellular matrix (ECM) that are known to interact with AAV2 capsid proteins.[38,39] Syndecans and glypicans are cell-membrane-associated HSPGs previously identified as primary receptors for AAV2, which allow the vector to dock and interact with co-receptors for cell entry.[40] Perlecans, which are ECM-related HSPGs, store AAV2 to facilitate its presentation to receptors for cell entry.[41] In the present study, mRNA levels of syndecan-4 and glypican-1 showed significant (1.2-fold) increases in the mouse retinas of 2 months of diabetes, while perlecan levels were decreased after 2 months of STZ treatment. Previous studies have shown that HSPG may be downregulated in DR, especially perlecans, which may in turn be responsible for increased capillary permeability in diabetic retinas.[42,43] However, in contrast to what was shown in our study, Díaz-Lezama et al.[16] recently demonstrated that mRNA levels of perlecans in the retina, along with those of syndecans and glypicans, were significantly increased in diabetic rats 4 weeks after STZ treatment. Such discrepancies suggest that HSPG expression in the retina may change with DR progression, which in turn may affect the efficacy of vector transduction. The mRNA levels of three co-receptors for AAV2 (FGFR1, αvβ5, and HGFR) were also significantly increased in diabetic mice after 2 months of STZ treatment, further supporting the enhanced AAV2 transduction seen in the present study. While much less is known about receptors and co-receptors for AAV9, N-linked galactose has been identified as a primary receptor for AAV9, and laminin receptors have been shown to act as co-receptors.[44,45] Our results showed significantly increased expression of laminin receptors in diabetic mouse retinas, which was consistent with previous reports showing upregulated expression of laminin receptors in an ischemic retinopathy mouse model.[46,47] Taken together, these findings suggested that increased levels of primary receptors and co-receptors are in part responsible for the enhanced AAV2 and 9 transduction.

In addition to the increased expression levels of specific receptors for AAV2 and AAV9, which could have direct correlations with the enhanced transduction of vectors, there are other major rate-limiting

Figure 4. Representative Cross-Section of Retinal Images of AAV2-EGFP-Administered Diabetic Mice Immunostained with Six Different Antibodies (GS, CD31, iba-1, NeuN, PKCα, and Calbindin; Red) and EGFP (Green)

Transverse retinal sections of 2-month-old diabetic mice revealed effective AAV2 transduction into Müller cells (GS; A1–A3 and B) and microglias (iba-1; E1–E3 and F) in 2-month-old diabetic mouse retinas, while vascular endothelial cells (CD31; C1–C3 and D) did not show any signs of AAV2 transduction in vector-injected eyes. Additionally, the EGFP expression co-localized with NeuN (G1–G3 and H), PKCα (I1–I3 and J), calbindin (K1–K3 and L), and calretinin (M1–M3 and N), indicating successful vector transduction in various inner retinal cells. INL, inner nuclear layer; ONL, outer nuclear layer. (A1–A3, C1–C3, E1–E3, G1–G3, I1–I3, K1–K3, and M1–M3) Scale bars, 100 μm; and (B, D, F, H, J, L, and N) scale bars, 40 μm.

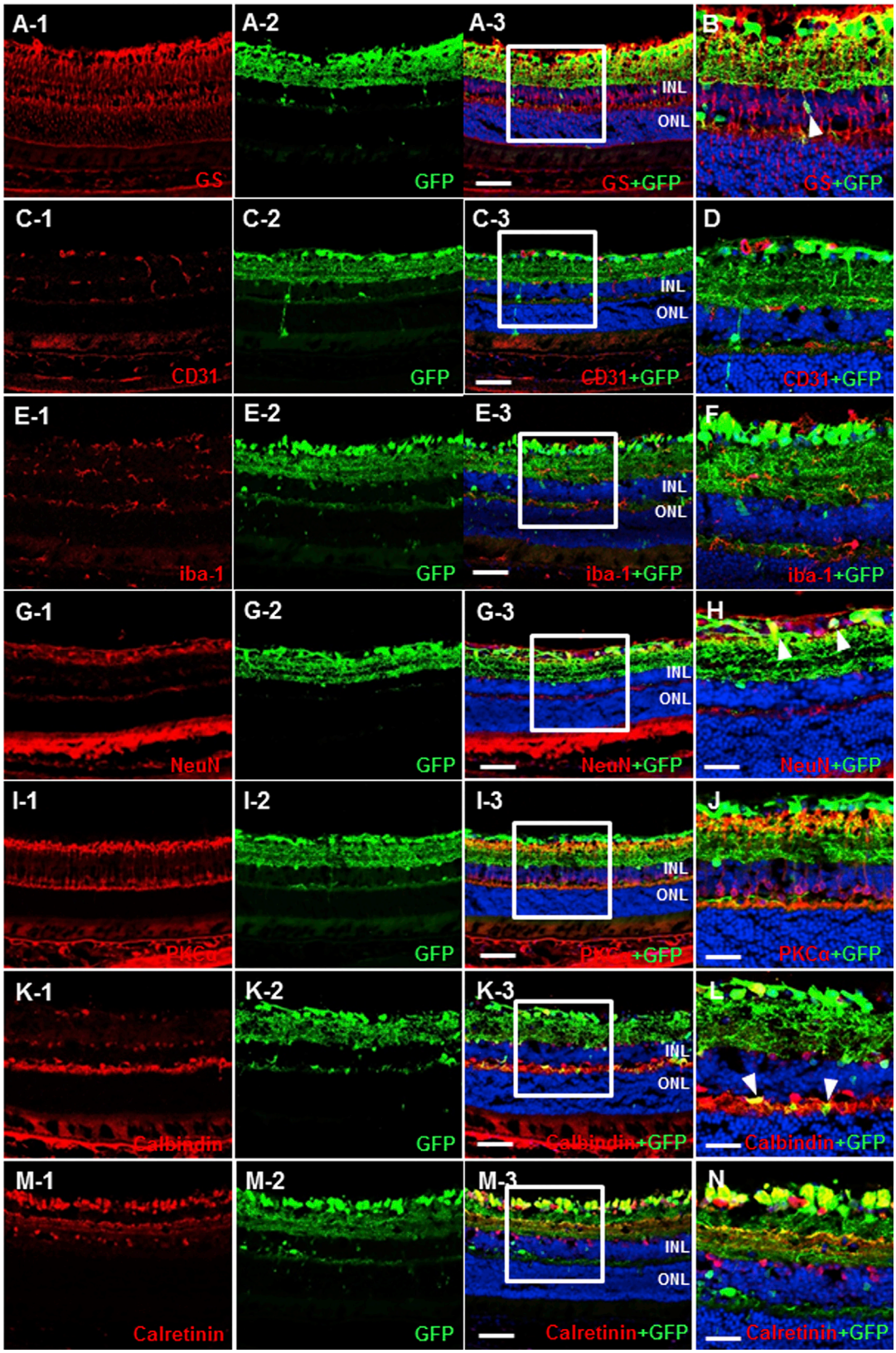

(legend on next page)

steps during AAV transduction of retinal cells. Nuclear uptake and the capsid uncoating process are necessary during vector transduction, and second-strand DNA synthesis after entering the cell is another important rate-limiting step.[48–50] Any alteration of these important steps in DR retinas may affect the transduction efficacy. Moreover, simple manipulations to the retina may enhance transduction efficiency in diabetic retinas. Removal of the internal limiting membrane[51,52] and laser pretreatment[14] have previously been reported to enhance AAV transduction efficiency in rodent retinas, and further studies are needed to reveal their role in enhancing AAV transduction in DR.

In this study, we used similar low concentration of viral vectors compared to previous studies (1.0×10^{10} viral genome [vg]/mL). While subretinal administration of AAV showed no significant adverse events related to ocular inflammation in many previous clinical trials, recent phase I and IIa trial of retinal AAV8-RS1 gene therapy for X-Linked retinoschisis reported that dose-related inflammatory response may occur following intravitreal delivery of AAV vector.[53] To prevent such possible adverse events, lower concentration of AAV compared to the conventionally used dose should be evaluated for its transduction efficiency in the retina. Previous studies using intravitreal delivery of a low dose of AAV ($10^9 - 10^{10}$ vg/mL) have shown sufficient transduction in various conditions of the retina.[14,54,55] Hence, we used similar AAV concentration to minimize unexpected adverse events due to unnecessarily high vector dose usage in this study. However, further studies are needed to find most appropriate concentration of the vector with the highest transduction efficacy and the minimal inflammatory response.

In conclusion, we demonstrated in this study that the transduction efficiencies of AAV2 and AAV9 were enhanced in diabetic mice after 2 months of STZ treatment, but not those of AAV5 and AAV8. Additionally, short duration STZ treatment (2 weeks) did not have a significant effect on the transduction patterns of AAV vectors in the retina, while 2 months of STZ treatment induced significantly enhanced vector transduction, indicating that certain retinal structural changes are needed to favor AAV transduction in diabetic retinas. Our results suggest that AAV2 and AAV9 may be the most appropriate viral vector for treating DR, and prolonged diabetic state and corresponding changes of the retina may improve transduction efficiency of intravitreally delivered AAV vectors. The findings of this study improve the current understanding of ocular gene therapy in DR and may aid future studies in identifying the most suitable AAV serotypes for gene therapy for DR.

MATERIALS AND METHODS

Animals

Thirty male C57BL/6J mice, aged 8 weeks (Orient Bio, Sungnam, Republic of Korea), were used in this study. All mice were reared in standard conditions under a 12-hr light and dark cycle. Animal care and experiments were conducted in accordance with the Association for Research in Vision and Ophthalmology Statement for the Use of Animals in Ophthalmic and Vision Research and overseen by the Institutional Animal Care and Use Committee of Soonchunhyang University Hospital, Bucheon, Republic of Korea.

Development of Diabetic Mice

Animals were injected with an intraperitoneal (i.p.) injection of STZ (150 mg/kg in sodium citrate buffer) (Sigma-Aldrich, St. Louis, MO, USA) or vehicle after 4 hr of fasting. To avoid sudden hypoglycemia after STZ injection, 10% sucrose water was supplied overnight. Mice with blood glucose levels >250 mg/dL at 48 hr were considered diabetic, and blood glucose measurements were performed weekly to check for persistent hyperglycemia.

Intravitreal AAV Administration

After 2 weeks or 2 months of i.p. STZ injection, intravitreal AAV injection was performed into the right eye under anesthesia using a mixture of 40 mg/kg zolazepam and tiletamine (Zoletil; Virbac, Carros Cedex, France) and 5 mg/kg xylazine (Rompun; Bayer Healthcare, Leverkusen, Germany) after pupil dilation with a mixture of 0.5% tropicamide and 0.5% phenylephrine hydrochloride (HCL) (Tropherine Eye Drops; Hanmi Pharm, Seoul, Republic of Korea). A sclerotomy was created using a sharp 30G needle tip prior to vector administration at approximately 0.5–1 mm posterior to the limbus and 1 μL of AAV2-EGFP, AAV5-EGFP, AAV8-EGFP, and AAV9-EGFP (1.0×10^{10} vg/mL) supplied by CdmoGen (Cheongju, Republic of Korea) were used for injection. Intravitreal injection was performed using a NanoFil syringe fitted with a 35G blunt needle (World Precision Instruments, Sarasota, FL, USA), and the fundus was directly visualized with a surgical microscope and a small plastic ring filled with 0.5% methylcellulose on the cornea (GenTeal; Novartis, Basel, Switzerland) during the injection procedure. Ten mice in each group, i.e., nondiabetic control, 2-week STZ injection, and 2-month STZ injection groups, were injected with each AAV serotype.

Tissue Processing and Immunohistochemistry

Tissue processing for immunohistochemistry was performed according to previously published procedures.[14,22] In brief, at 1 month after AAV administration, mice were deeply anesthetized with a 4:1 mixture of zolazepam and tiletamine and xylazine, and intracardial perfusion was performed with 0.1 M PBS containing 150 U/mL

Figure 5. Transverse Sectional Images of AAV9-EGFP-Administered Diabetic Mice Immunostained with EGFP (Green) and Six Different Antibodies (GS, CD31, iba-1, NeuN, PKCα, and Calbindin; Red)

In 2-month-old diabetic mice with intravitreal AAV9 injection, EGFP expression co-localized only with Müller cells (GS; A1–A3 and B), RGCs (NeuN; G1–G3 and H), and horizontal cells (calbindin; K1–K3 and L), whereas endothelial cells (CD31; C1–C3 and D), microglia (iba-1; E1–E3 and F), bipolar cells (PKCα; I1–I3 and J), and amacrine cells (calretinin; M1–M3 and N) did not show any EGFP expression. INL, inner nuclear layer; ONL, outer nuclear layer. (A1–A3, C1–C3, E1–E3, G1–G3, I1–I3, K1–K3, and M1–M3) scale bars, 100 μm; and (B, D, F, H, J, L, and N) scale bars, 40 μm.

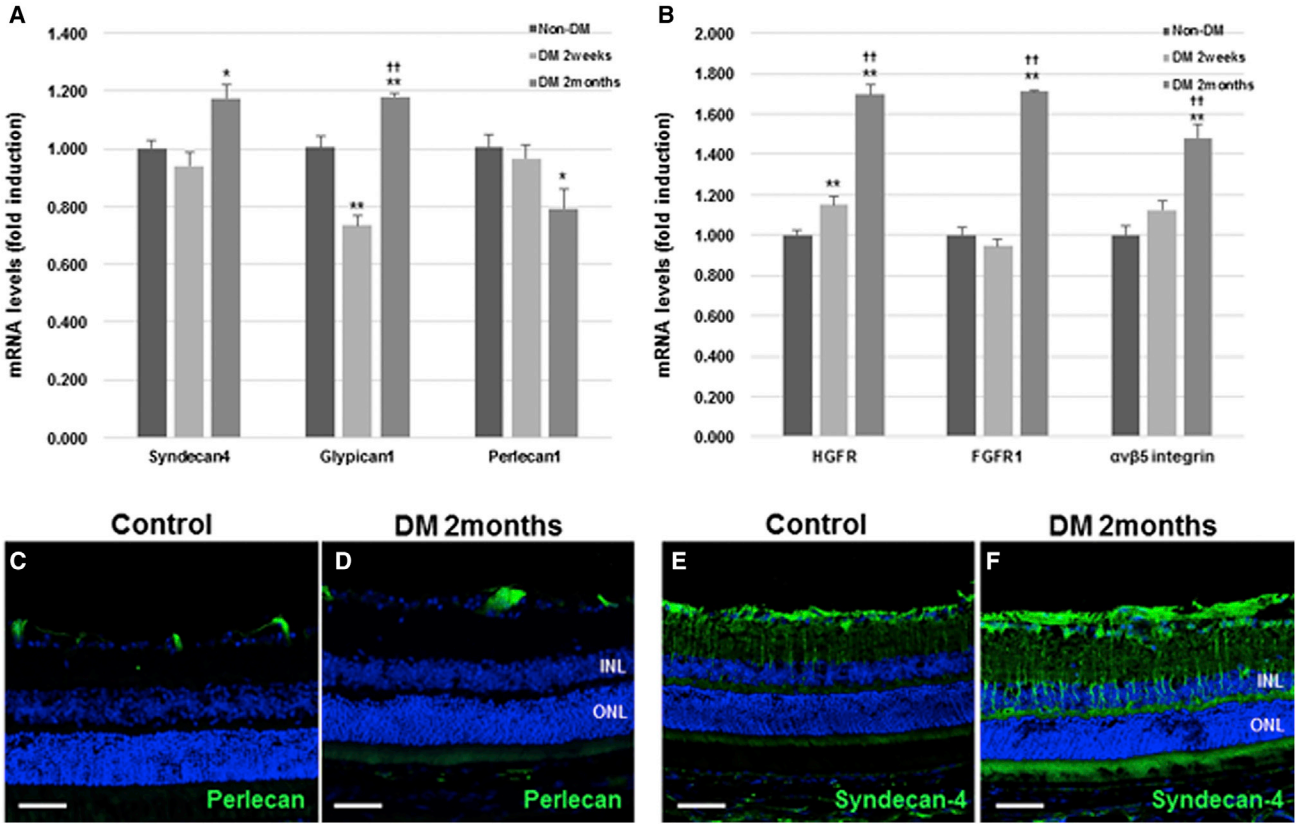

Figure 6. Expression of Primary Receptors and Co-receptors of AAV2 in Control and 2-Month-Old Diabetic Mouse Retinas

The mRNA levels of primary receptors (syndecan, glypican, and perlecan) and co-receptors (FGFR1, αvβ5 integrin, and HGFR) for AAV2 were evaluated using retinas from a normal control and a 2-month-old diabetic mouse. The expressions of syndecan-4, glypican-1 (A), and all three co-receptors for AAV2 (B) were significantly increased in 2-month-old diabetic mouse retinas compared to the non-diabetic controls, whereas the perlecan-1 level was significantly decreased in the diabetic mouse retinas (A and B). Results are expressed as the mean ± SEM. *$p < 0.05$, **$p < 0.01$ compared to the normal group, tested by the Mann-Whitney U test. $^{\dagger}p < 0.05$, $^{\dagger\dagger}p < 0.01$ compared to 2-week-old diabetic mice, tested by the Mann-Whitney U test. INL, inner nuclear layer; ONL, outer nuclear layer. Scale bars, 100 μm.

heparin, followed by 4% paraformaldehyde (PFA) in 0.1 M PBS. Eyes were then enucleated, and the anterior segment and lens were removed and post-fixed in 4% PFA. Eyecups were examined and photographed using an Axioplan microscope at 50× magnification (Carl Zeiss, Oberkochen, Germany). A monochromatic charge-coupled device camera (Axio-CamMRm; Carl Zeiss) and Axiovision image-capture software (Carl Zeiss) were used to obtain the images. After images were captured, eyecups were incubated in 30% sucrose in PBS overnight and embedded sagittally in OCT compound. Then, 10-μm serial sections were cut from the eyecups and mounted on microscope slides (Histobond; Marienfeld-Superior, Lauda-Königshofen, Germany). For retinal whole-mount preparation, eyes from each group were dissected into posterior eyecups and were then fixed in 4% PFA and prepared as flattened whole mounts with four equidistant cuts.

For immunohistochemistry, transverse tissue sections were blocked with 0.1% Triton X-100 in 5% goat serum for 1 hr. Sections were then incubated with various primary antibodies overnight at 4°C. The primary antibodies used in this study are described in Table S1. EGFP was visualized using an anti-GFP antibody (1:200, ab6556; Abcam, Cambridge, UK). The samples were then incubated with the appropriate secondary antibodies for 1 hr at room temperature, and DAPI (0.1 mg/mL; Sigma-Aldrich) stain was used to label cell nuclei with 3 min of incubation. The secondary antibodies used in this study were as follows: Alexa Fluor 488 anti-rabbit, Alexa Fluor 488 anti-mouse, and Alexa Fluor 568 anti-mouse (1:2,000; Molecular Probes, Grand Island, NY, USA). For RCA I immunohistochemistry (1:500, RL-1082; Vector Laboratories, Burlingame, CA, USA), 2-hr incubation at room temperature was performed without applying secondary antibody. The sections were examined by confocal microscopy (LSM510 Meta; Carl Zeiss).

qRT-PCR

After the animals had been deeply anesthetized, the eyeball was enucleated, and the cornea, lens, and retinal pigment epithelium (RPE)-choroid complex were removed. Total RNA was extracted from the neural retina without the RPE-choroid complex using

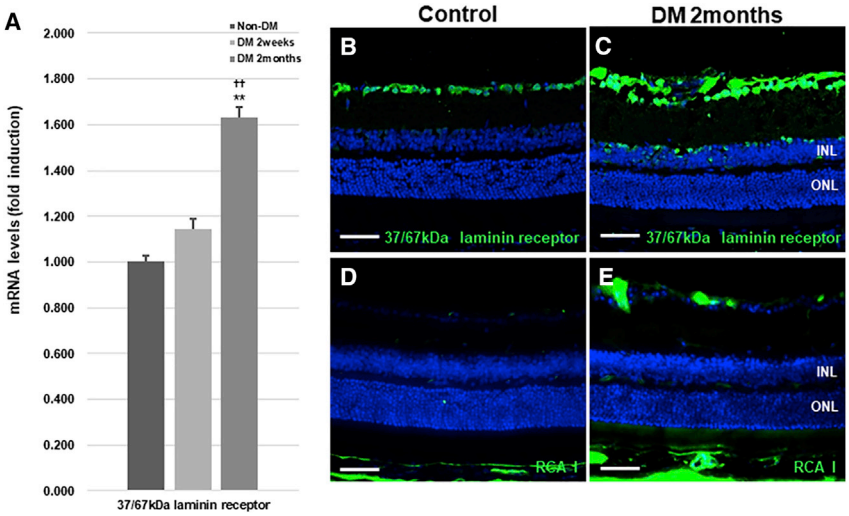

Figure 7. Immunoreactivity and mRNA Levels of AAV9 Receptors in Control and 2-Month-Old Diabetic Mouse Retinas

The mRNA level of 37- and 67-kDa laminin receptors, an AAV9 receptor, was significantly increased in 2-month-old diabetic mouse retinas compared with nondiabetic controls (A). Consistent immunostaining of the 37- and 67-kDa laminin receptor also demonstrated enhanced expression of the receptor in the RGC layer as well as the INL in 2-month-old diabetic mouse retinas (C) compared to nondiabetic controls (B). RCA I expression was also markedly increased in 2-month-old diabetic mouse retinas (E) compared to the nondiabetic control (D). The results are expressed as the mean ± SEM. *$p < 0.05$ and **$p < 0.01$ compared to the control group, tested by the Mann-Whitney U test. $^{\dagger}p < 0.05$ and $^{\dagger\dagger}p < 0.01$ compared to 2-week-old diabetic mouse, also tested by the Mann-Whitney U test. INL, inner nuclear layer; ONL, outer nuclear layer. Scale bars, 100 μm.

TRIzol reagent (Invitrogen, Tokyo, Japan). RNA (2 μg) was reverse transcribed into cDNA using Superscript III (Invitrogen), and qRT-PCR for mRNA levels was performed using SYBR Green kits (Invitrogen). Fold changes in mRNA expression were determined using the $2^{-\Delta\Delta Ct}$ method, normalizing the results to the expression of the control *GAPDH*. PCR was conducted in triplicate using pairs of the primers listed in Table S2.

Image Analysis and Statistical Analysis

Fluorescence intensity of each eyecup image was measured using ImageJ software (NIH, Bethesda, MD, USA), and relative fluorescence intensity for each image was calculated as the fluorescence intensity relative to the averaged fluorescence intensity of the control eyes. The Wilcoxon signed-rank test was used to quantitatively compare fluorescence intensities among the experimental groups.

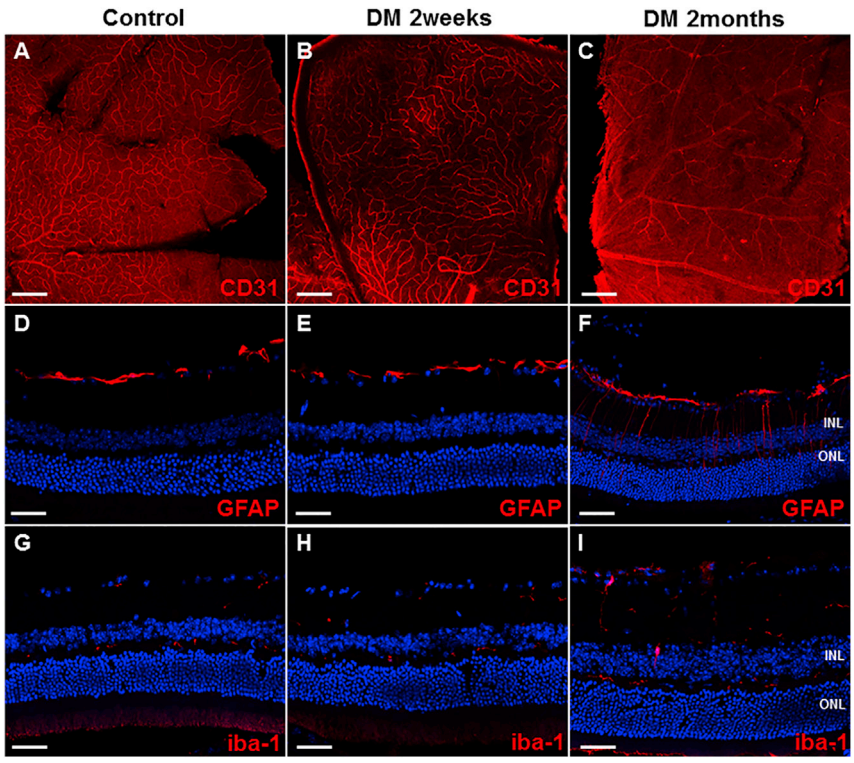

Figure 8. Retinal Whole-Mount and Cross-Sectional Images Immunostained with CD31, GFAP, and iba-1 (Red)

In 2-month-old diabetic mouse retinas, markedly increased avascular area was observed (CD31; C) compared to the non-diabetic control (A) and 2-week-old diabetic mouse retinas (B). Also, increased GFAP expression, mainly in the inner retinal layers, was detected in 2-month-old diabetic mouse retinas (F) compared to the nondiabetic control (D) and 2-week-old diabetic mouse retinas (F) and iba-1 (G–I). As for microglial cell activation, minimal iba-1 expression was observed in nondiabetic control (G) and 2-week-old diabetic mouse retinas (H), while increased expression was seen in 2-month-old diabetic mouse retinas (I). INL, inner nuclear layer; ONL, outer nuclear layer. (A–C) scale bars, 100 μm; and (D–I) scale bars, 50 μm.

Statistical analyses were conducted using SPSS for Windows software (ver. 20.0; SPSS, Chicago, IL, USA). A p value < 0.05 was considered statistically significant.

SUPPLEMENTAL INFORMATION

Supplemental Information includes two tables and can be found with this article online at https://doi.org/10.1016/j.omtm.2018.11.008.

AUTHOR CONTRIBUTIONS

Conceptualization, T.K.P.; Methodology, T.K.P., S.H.L., J.Y.Y.; Validation, J.Y.Y., T.K.P.; Investigation, S.H.L., J.Y.Y., S.M., H.Y.P.; Resources, T.K.P., K.P.; Writing – Original Draft, S.H.L.; Writing – Review & Editing, T.K.P., S.H.L., J.Y.Y.; Visualization, S.H.L., J.Y.Y; Supervision, T.K.P. and K.P.; Project Administration, T.K.P.; Funding Acquisition, T.K.P.

CONFLICTS OF INTEREST

No potential conflict of interest exists for all authors.

ACKNOWLEDGMENTS

This research was supported by a grant from the Korea Health Technology R&D Project through the Korea Health Industry Development Institute (KHIDI), funded by the Ministry of Health and Welfare (grant number HI17C0966), and also partially supported by the Soonchunhyang University research fund.

REFERENCES

1. The Diabetic Retinopathy Study Research Group (1981). Photocoagulation treatment of proliferative diabetic retinopathy. Clinical application of Diabetic Retinopathy Study (DRS) findings, DRS Report Number 8. Ophthalmology *88*, 583–600.

2. McDonald, H.R., and Schatz, H. (1985). Visual loss following panretinal photocoagulation for proliferative diabetic retinopathy. Ophthalmology *92*, 388–393.

3. Fong, D.S. (2002). Changing times for the management of diabetic retinopathy. Surv. Ophthalmol. *47* (*Suppl 2*), S238–S245.

4. Boyer, D.S., Hopkins, J.J., Sorof, J., and Ehrlich, J.S. (2013). Anti-vascular endothelial growth factor therapy for diabetic macular edema. Ther. Adv. Endocrinol. Metab. *4*, 151–169.

5. Bainbridge, J.W., Smith, A.J., Barker, S.S., Robbie, S., Henderson, R., Balaggan, K., Viswanathan, A., Holder, G.E., Stockman, A., Tyler, N., et al. (2008). Effect of gene therapy on visual function in Leber's congenital amaurosis. N. Engl. J. Med. *358*, 2231–2239.

6. Hauswirth, W.W., Aleman, T.S., Kaushal, S., Cideciyan, A.V., Schwartz, S.B., Wang, L., Conlon, T.J., Boye, S.L., Flotte, T.R., Byrne, B.J., and Jacobson, S.G. (2008). Treatment of leber congenital amaurosis due to RPE65 mutations by ocular subretinal injection of adeno-associated virus gene vector: short-term results of a phase I trial. Hum. Gene Ther. *19*, 979–990.

7. Maguire, A.M., Simonelli, F., Pierce, E.A., Pugh, E.N., Jr., Mingozzi, F., Bennicelli, J., Banfi, S., Marshall, K.A., Testa, F., Surace, E.M., et al. (2008). Safety and efficacy of gene transfer for Leber's congenital amaurosis. N. Engl. J. Med. *358*, 2240–2248.

8. Xu, H., Zhang, L., Gu, L., Lu, L., Gao, G., Li, W., Xu, G., Wang, J., Gao, F., Xu, J.Y., et al. (2014). Subretinal delivery of AAV2-mediated human erythropoietin gene is protective and safe in experimental diabetic retinopathy. Invest. Ophthalmol. Vis. Sci. *55*, 1519–1530.

9. Dominguez, J.M., 2nd, Hu, P., Caballero, S., Moldovan, L., Verma, A., Oudit, G.Y., Li, Q., and Grant, M.B. (2016). Adeno-Associated Virus Overexpression of Angiotensin-Converting Enzyme-2 Reverses Diabetic Retinopathy in Type 1 Diabetes in Mice. Am. J. Pathol. *186*, 1688–1700.

10. Birke, M.T., Lipo, E., Adhi, M., Birke, K., and Kumar-Singh, R. (2014). AAV-mediated expression of human PRELP inhibits complement activation, choroidal neovascularization and deposition of membrane attack complex in mice. Gene Ther. *21*, 507–513.

11. Askou, A.L., Pournaras, J.A., Pihlmann, M., Svalgaard, J.D., Arsenijevic, Y., Kostic, C., Bek, T., Dagnaes-Hansen, F., Mikkelsen, J.G., Jensen, T.G., and Corydon, T.J. (2012). Reduction of choroidal neovascularization in mice by adeno-associated virus-delivered anti-vascular endothelial growth factor short hairpin RNA. J. Gene Med. *14*, 632–641.

12. Maclachlan, T.K., Lukason, M., Collins, M., Munger, R., Isenberger, E., Rogers, C., Malatos, S., Dufresne, E., Morris, J., Calcedo, R., et al. (2011). Preclinical safety evaluation of AAV2-sFLT01- a gene therapy for age-related macular degeneration. Mol. Ther. *19*, 326–334.

13. Igarashi, T., Miyake, K., Asakawa, N., Miyake, N., Shimada, T., and Takahashi, H. (2013). Direct comparison of administration routes for AAV8-mediated ocular gene therapy. Curr. Eye Res. *38*, 569–577.

14. Lee, S.H., Colosi, P., Lee, H., Ohn, Y.H., Kim, S.W., Kwak, H.W., and Park, T.K. (2014). Laser photocoagulation enhances adeno-associated viral vector transduction of mouse retina. Hum. Gene Ther. Methods *25*, 83–91.

15. Lee, J.Y., Hwang, Y., Kim, J.H., Kim, Y.S., Jung, B.K., Kim, P., and Lee, H. (2016). In Vivo Fluorescence Retinal Imaging Following AAV2-Mediated Gene Delivery in the Rat Retina. Invest. Ophthalmol. Vis. Sci. *57*, 3390–3396.

16. Díaz-Lezama, N., Wu, Z., Adán-Castro, E., Arnold, E., Vázquez-Membrillo, M., Arredondo-Zamarripa, D., Ledesma-Colunga, M.G., Moreno-Carranza, B., Martinez de la Escalera, G., Colosi, P., and Clapp, C. (2016). Diabetes enhances the efficacy of AAV2 vectors in the retina: therapeutic effect of AAV2 encoding vasoinhibin and soluble VEGF receptor 1. Lab. Invest. *96*, 283–295.

17. Li, H.L., Zheng, X.Z., Wang, H.P., Li, F., Wu, Y., and Du, L.F. (2009). Ultrasound-targeted microbubble destruction enhances AAV-mediated gene transfection in human RPE cells in vitro and rat retina in vivo. Gene Ther. *16*, 1146–1153.

18. Ideno, J., Mizukami, H., Kakehashi, A., Saito, Y., Okada, T., Urabe, M., Kume, A., Kuroki, M., Kawakami, M., Ishibashi, S., and Ozawa, K. (2007). Prevention of diabetic retinopathy by intraocular soluble flt-1 gene transfer in a spontaneously diabetic rat model. Int. J. Mol. Med. *19*, 75–79.

19. Ramírez, M., Wu, Z., Moreno-Carranza, B., Jeziorski, M.C., Arnold, E., Díaz-Lezama, N., Martínez de la Escalera, G., Colosi, P., and Clapp, C. (2011). Vasoinhibin gene transfer by adenoassociated virus type 2 protects against VEGF- and diabetes-induced retinal vasopermeability. Invest. Ophthalmol. Vis. Sci. *52*, 8944–8950.

20. Shyong, M.P., Lee, F.L., Kuo, P.C., Wu, A.C., Cheng, H.C., Chen, S.L., Tung, T.H., and Tsao, Y.P. (2007). Reduction of experimental diabetic vascular leakage by delivery of angiostatin with a recombinant adeno-associated virus vector. Mol. Vis. *13*, 133–141.

21. Verma, A., Shan, Z., Lei, B., Yuan, L., Liu, X., Nakagawa, T., Grant, M.B., Lewin, A.S., Hauswirth, W.W., Raizada, M.K., and Li, Q. (2012). ACE2 and Ang-(1-7) confer protection against development of diabetic retinopathy. Mol. Ther. *20*, 28–36.

22. Lee, S.H., Kim, Y.S., Nah, S.K., Kim, H.J., Park, H.Y., Yang, J.Y., Park, K., and Park, T.K. (2018). Transduction Patterns of Adeno-associated Viral Vectors in a Laser-Induced Choroidal Neovascularization Mouse Model. Mol. Ther. Methods Clin. Dev. *9*, 90–98.

23. Lee, S.H., Kong, Y.J., Lyu, J., Lee, H., Park, K., and Park, T.K. (2015). Laser Photocoagulation Induces Transduction of Retinal Pigment Epithelial Cells by Intravitreally Administered Adeno-Associated Viral Vectors. Hum. Gene Ther. Methods *26*, 159–161.

24. Hickey, D.G., Edwards, T.L., Barnard, A.R., Singh, M.S., de Silva, S.R., McClements, M.E., Flannery, J.G., Hankins, M.W., and MacLaren, R.E. (2017). Tropism of engineered and evolved recombinant AAV serotypes in the rd1 mouse and ex vivo primate retina. Gene Ther. *24*, 787–800.

25. Wiley, L.A., Burnight, E.R., Kaalberg, E.E., Jiao, C., Riker, M.J., Halder, J.A., Luse, M.A., Han, I.C., Russell, S.R., Sohn, E.H., et al. (2018). Assessment of Adeno-Associated Virus Serotype Tropism in Human Retinal Explants. Hum. Gene Ther. *29*, 424–436.

26. Watanabe, S., Sanuki, R., Ueno, S., Koyasu, T., Hasegawa, T., and Furukawa, T. (2013). Tropisms of AAV for subretinal delivery to the neonatal mouse retina and

its application for in vivo rescue of developmental photoreceptor disorders. PLoS ONE *8*, e54146.

27. Harvey, A.R., Hellström, M., and Rodger, J. (2009). Gene therapy and transplantation in the retinofugal pathway. Prog. Brain Res. *175*, 151–161.
28. Zhang, J., Wu, Y., Jin, Y., Ji, F., Sinclair, S.H., Luo, Y., Xu, G., Lu, L., Dai, W., Yanoff, M., et al. (2008). Intravitreal injection of erythropoietin protects both retinal vascular and neuronal cells in early diabetes. Invest. Ophthalmol. Vis. Sci. *49*, 732–742.
29. Rungger-Brändle, E., Dosso, A.A., and Leuenberger, P.M. (2000). Glial reactivity, an early feature of diabetic retinopathy. Invest. Ophthalmol. Vis. Sci. *41*, 1971–1980.
30. Xu, X., Zhu, Q., Xia, X., Zhang, S., Gu, Q., and Luo, D. (2004). Blood-retinal barrier breakdown induced by activation of protein kinase C via vascular endothelial growth factor in streptozotocin-induced diabetic rats. Curr. Eye Res. *28*, 251–256.
31. Qaum, T., Xu, Q., Joussen, A.M., Clemens, M.W., Qin, W., Miyamoto, K., Hassessian, H., Wiegand, S.J., Rudge, J., Yancopoulos, G.D., and Adamis, A.P. (2001). VEGF-initiated blood-retinal barrier breakdown in early diabetes. Invest. Ophthalmol. Vis. Sci. *42*, 2408–2413.
32. Robinson, R., Barathi, V.A., Chaurasia, S.S., Wong, T.Y., and Kern, T.S. (2012). Update on animal models of diabetic retinopathy: from molecular approaches to mice and higher mammals. Dis. Model. Mech. *5*, 444–456.
33. Olivares, A.M., Althoff, K., Chen, G.F., Wu, S., Morrisson, M.A., DeAngelis, M.M., and Haider, N. (2017). Animal Models of Diabetic Retinopathy. Curr. Diab. Rep. *17*, 93.
34. Barber, A.J., Lieth, E., Khin, S.A., Antonetti, D.A., Buchanan, A.G., and Gardner, T.W. (1998). Neural apoptosis in the retina during experimental and human diabetes. Early onset and effect of insulin. J. Clin. Invest. *102*, 783–791.
35. Zeng, X.X., Ng, Y.K., and Ling, E.A. (2000). Neuronal and microglial response in the retina of streptozotocin-induced diabetic rats. Vis. Neurosci. *17*, 463–471.
36. Asnaghi, V., Gerhardinger, C., Hoehn, T., Adeboje, A., and Lorenzi, M. (2003). A role for the polyol pathway in the early neuroretinal apoptosis and glial changes induced by diabetes in the rat. Diabetes *52*, 506–511.
37. Kohzaki, K., Vingrys, A.J., and Bui, B.V. (2008). Early inner retinal dysfunction in streptozotocin-induced diabetic rats. Invest. Ophthalmol. Vis. Sci. *49*, 3595–3604.
38. Boye, S.L., Bennett, A., Scalabrino, M.L., McCullough, K.T., Van Vliet, K., Choudhury, S., Ruan, Q., Peterson, J., Agbandje-McKenna, M., and Boye, S.E. (2016). Impact of Heparan Sulfate Binding on Transduction of Retina by Recombinant Adeno-Associated Virus Vectors. J. Virol. *90*, 4215–4231.
39. Woodard, K.T., Liang, K.J., Bennett, W.C., and Samulski, R.J. (2016). Heparan Sulfate Binding Promotes Accumulation of Intravitreally Delivered Adeno-associated Viral Vectors at the Retina for Enhanced Transduction but Weakly Influences Tropism. J. Virol. *90*, 9878–9888.
40. Kern, A., Schmidt, K., Leder, C., Müller, O.J., Wobus, C.E., Bettinger, K., Von der Lieth, C.W., King, J.A., and Kleinschmidt, J.A. (2003). Identification of a heparin-binding motif on adeno-associated virus type 2 capsids. J. Virol. *77*, 11072–11081.
41. Vivès, R.R., Lortat-Jacob, H., and Fender, P. (2006). Heparan sulphate proteoglycans and viral vectors : ally or foe? Curr. Gene Ther. *6*, 35–44.
42. Bollineni, J.S., Alluru, I., and Reddi, A.S. (1997). Heparan sulfate proteoglycan synthesis and its expression are decreased in the retina of diabetic rats. Curr. Eye Res. *16*, 127–130.
43. Hammes, H.P., Weiss, A., Hess, S., Araki, N., Horiuchi, S., Brownlee, M., and Preissner, K.T. (1996). Modification of vitronectin by advanced glycation alters functional properties in vitro and in the diabetic retina. Lab. Invest. *75*, 325–338.
44. Shen, S., Bryant, K.D., Brown, S.M., Randell, S.H., and Asokan, A. (2011). Terminal N-linked galactose is the primary receptor for adeno-associated virus 9. J. Biol. Chem. *286*, 13532–13540.
45. Akache, B., Grimm, D., Pandey, K., Yant, S.R., Xu, H., and Kay, M.A. (2006). The 37/67-kilodalton laminin receptor is a receptor for adeno-associated virus serotypes 8, 2, 3, and 9. J. Virol. *80*, 9831–9836.
46. Stitt, A.W., McKenna, D., Simpson, D.A., Gardiner, T.A., Harriott, P., Archer, D.B., and Nelson, J. (1998). The 67-kd laminin receptor is preferentially expressed by proliferating retinal vessels in a murine model of ischemic retinopathy. Am. J. Pathol. *152*, 1359–1365.
47. Gebarowska, D., Stitt, A.W., Gardiner, T.A., Harriott, P., Greer, B., and Nelson, J. (2002). Synthetic peptides interacting with the 67-kd laminin receptor can reduce retinal ischemia and inhibit hypoxia-induced retinal neovascularization. Am. J. Pathol. *160*, 307–313.
48. Ding, W., Zhang, L., Yan, Z., and Engelhardt, J.F. (2005). Intracellular trafficking of adeno-associated viral vectors. Gene Ther. *12*, 873–880.
49. Thomas, C.E., Storm, T.A., Huang, Z., and Kay, M.A. (2004). Rapid uncoating of vector genomes is the key to efficient liver transduction with pseudotyped adeno-associated virus vectors. J. Virol. *78*, 3110–3122.
50. Ferrari, F.K., Samulski, T., Shenk, T., and Samulski, R.J. (1996). Second-strand synthesis is a rate-limiting step for efficient transduction by recombinant adeno-associated virus vectors. J. Virol. *70*, 3227–3234.
51. Dalkara, D., Kolstad, K.D., Caporale, N., Visel, M., Klimczak, R.R., Schaffer, D.V., and Flannery, J.G. (2009). Inner limiting membrane barriers to AAV-mediated retinal transduction from the vitreous. Mol. Ther. *17*, 2096–2102.
52. Teo, K.Y.C., Lee, S.Y., Barathi, A.V., Tun, S.B.B., Tan, L., and Constable, I.J. (2018). Surgical Removal of Internal Limiting Membrane and Layering of AAV Vector on the Retina Under Air Enhances Gene Transfection in a Nonhuman Primate. Invest. Ophthalmol. Vis. Sci. *59*, 3574–3583.
53. Cukras, C., Wiley, H.E., Jeffrey, B.G., Sen, H.N., Turriff, A., Zeng, Y., Vijayasarathy, C., Marangoni, D., Ziccardi, L., Kjellstrom, S., et al. (2018). Retinal AAV8-RS1 Gene Therapy for X-Linked Retinoschisis: Initial Findings from a Phase I/IIa Trial by Intravitreal Delivery. Mol. Ther *26*, 2282–2294.
54. Park, T.K., Lee, S.H., Choi, J.S., Nah, S.K., Kim, H.J., Park, H.Y., Lee, H., Lee, S.H.S., and Park, K. (2017). Adeno-Associated Viral Vector-Mediated mTOR Inhibition by Short Hairpin RNA Suppresses Laser-Induced Choroidal Neovascularization. Mol. Ther. Nucleic Acids *8*, 26–35.
55. Kay, C.N., Ryals, R.C., Aslanidi, G.V., Min, S.H., Ruan, Q., Sun, J., Dyka, F.M., Kasuga, D., Ayala, A.E., Van Vliet, K., et al. (2013). Targeting photoreceptors via intravitreal delivery using novel, capsid-mutated AAV vectors. PLoS ONE *8*, e62097.